NYO-9360

A FAST NEUTRON TIME OF FLIGHT SYSTEM FOR USE WITH CYCLOTRONS

by

H. W. Fulbright, J. W. Verba,
V. K. Deshpande, and A. K. Hamann

THE UNIVERSITY OF ROCHESTER

DEPARTMENT OF PHYSICS AND ASTRONOMY

ROCHESTER , NEW YORK

Report Number -- NYO-9360

A Fast Neutron Time of Flight System for use With Cyclotrons

by

H. W. Fulbright, J. W. Verba,
V. K. Deshpande, and A. K. Hamann

Department of Physics and Astronomy

University of Rochester

Rochester, New York

August 16, 1962

Contract Number AT(30-1)-875

DISCLAIMER

Introduction

Time of flight spectrometers for the study of neutrons emitted in charged particle reactions have become important in recent years, following the development of suitable photomultiplier tubes and electronic circuits for nanosecond (ns) timing measurements. The principle of operation is simple. The particles exciting the nuclear reactions in which the neutrons are produced fall on the target in bunches of the order of a nanosecond in width. The arrival of product neutrons at an organic scintillation counter (proton recoil) detector placed a few meters from the target gives signals which can be used to determine the flight time of the neutrons from target to detector. A time-reference pulse corresponding to the arrival of beam pulses at the target is required.

It is convenient to have the output data presented as a spectrum by a multi-channel device of some sort. Multi-channel pulse height analyzers are usually available in cyclotron or van de Graaff laboratories, and these can be used for data storage and presentation. In this case experimental equipment must be designed a) to produce a set of reference pulses corresponding to the arrival times of beam pulses at the target, and b) to convert the time differences between the neutron counter pulses and the corresponding reference pulses into proportional amplitudes of pulses artificially generated. The output pulse spectrum of the converter is fed directly into the multi-channel analyzer, so the output spectrum of the analyzer represents the distribution of neutrons in flight time.

In van de Graaff laboratories artificial modulation of the beam to produce sharp beam pulses is necessary. Typically the beam is electrostatically deflected by an electric field between two plates driven by a radio frequency oscillator operating at about 3 mc. so that it sweeps across the target in a few ns. Bunching techniques may also be employed. Reference pulses for timing can be derived either from the oscillator, or from a scintillation counter detector struck by the beam pulses, or from the pulses of target current, or from signals generated as the beam pulses pass through a hollow electrode before reaching the target.

In cyclotron laboratories the problem of obtaining a pulsed beam usually does not arise, because the beam of a conventional cyclotron is already naturally bunched. (A theory of cyclotron beam bunching together with experimental results given by Konradi[1] shows that bunching occurs within the first few turns.) In this case timing pulses can be obtained from the oscillator of the cyclotron itself, rather than from the beam-sweeping oscillator as in the van de Graaff case, or by any of the other methods mentioned above.

We have explored two of these possibilities, scintillation counter detection of beam pulses, and generation of reference pulses by use of voltages derived from the cyclotron oscillator. It has turned out that the more satisfactory source of reference information is the cyclotron oscillator, even though the phase

---

1. M. Konradi, R.S.I. 29, 840 (1958).

relationship between the emergent beam pulses and the oscillator voltage changes somewhat if the cyclotron magnet tuning is changed. In practice the stability of the cyclotron is so great that this causes very little trouble. There are two great practical advantages associated with the present system of obtaining reference pulses, a) the pulses are obtained in a way which makes them insensitive to beam current changes, and b) all reference pulses are smooth and identical in shape. In addition the system evolved is simple and has worked quite reliably. Figure 1 is a diagram of the overall setup of the system. Figure 2 is a block diagram of the electronic circuits.

The main purpose of what follows is to describe our time of flight system, including especially the reference pulse generator and the transistorized time-difference-to-pulse-height converter.

The Time to Pulse Height Converter

Figure 3 illustrates the principle of operation of the time to pulse height converter. A 6BN6 tube is normally non-conducting by virtue of a negative bias on its quadrature grid. If a 10 V positive square wave is applied to that grid the tube begins to conduct, and the condenser C begins to charge at a linear rate. If a 10 V negative square wave is applied to the control grid a short time later the tube is again cut off, and C begins to discharge logarithmically. In our circuit the generation of the positive (or"start") square wave is initiated by the neutron counter, and the generation of the subsequent negative (or "stop") square wave is due to the time reference signal derived from the cyclotron

oscillator. Thus the height of the negative signal is proportional to the time difference between the neutron pulse and the reference pulse. The time constant of the falling part of the output pulses is of the order of one microsecond.

Figure 4 shows the basic gated univibrator circuit used to generate the square waves, along with an inverter stage. This circuit will trigger directly on negative photomultiplier pulses bigger than about 0.3 volts.

Figure 5 shows the circuit diagram of the entire converter circuit. In addition to the two trigger circuits an interlock is provided which prevents a stop pulse from being applied to the 6BN6 unless there has recently arrived a start pulse. Except for the use of transistors this converter circuit is similar to that used by Cranberg and his collaborators at Los Alamos, and to a unit manufactured by the Eldorado Company.

Stop Trigger Pulse Generator

Figure 6 shows the circuit diagram of the stop trigger pulse generator. At the cyclotron oscillator end, the signal cable plugs into a connector, the shell of which is grounded to the oscillator house and the central electrode of which is connected to a short (10") antenna of No. 12 wire which extends inside the oscillator house to within a foot or two of the grid circuit of the oscillator. A signal consisting of a mixture of the fundamental and various harmonics of the oscillator frequency appears at the other end of the cable. A shunt section of cable (not shown in the diagram)

of variable length and variable terminating resistance is provided at the input to permit adjustment of the relative phases and amplitudes of the components. Sometimes two such shunt sections have been used.

The signal is fed into a gate circuit based on a shunt diode which is normally kept operating in the low resistance section of its characteristics curve by the plate current of a 6688 tube. Normally, therefore, no appreciable signal voltage appears across the diode. However, when the 6688 is made non-conducting by a negative square wave applied to its control grid, a positive signal is transmitted to the phase-inverting 404-A amplifier shown in Fig. 6, triggered by the start trigger pulse from the neutron detector. Thus stop trigger pulses emerge only after an event occurs in the neutron detector. (This feature makes the interlock circuit in the converter unit superfluous for present purposes.)

The output pulses are made about 10 volts high. Their rise time is of the order of 5 ns or less. See Fig. 7. When the cyclotron is operating at about 10 mc the shortest rise time available is about 3 ns, according to sampling oscilloscope observations. The square gate pulse is several tenths of a microsecond long, so several successive stop trigger pulses appear every time a neutron counter pulse triggers the circuit, but of course the first pulse stops the converter, so the other pulses have no effect.

Whenever the frequency of the cyclotron oscillator is changed (in order to change the energy of the beam) the shape of the stop trigger pulses must be checked on a fast oscilloscope, and if neces-

sary the shape must be adjusted by changing the tapped delay line and its termination. These adjustments ordinarily require less than a minute and are usually not necessary for small changes of frequency. This simple stop trigger pulse generator has proven entirely satisfactory in several years of use.

The Overall Circuit Hookup

Figure 2 shows a block diagram of the hookup of the various electronic units. Several fast amplifiers and delay lines are shown in various trigger lines. Their functions are obvious. The gain of the fast amplifiers supplying the signal which opens the gate circuit of the stop pulse generator must be great enough to ensure that the gate will be opened by any counter pulse big enough to start the converter circuit and the slow discriminator circuit, otherwise large, unstopped, pulses may be recorded, and in addition distortion of the spectrum will occur, because some of the smaller pulses will not be effective.

In addition a slow amplifier and attenuator and single channel pulse height discriminator are shown connected to the output of the neutron detector. The output of the discriminator is often used to control registration of counts in the multi-channel analyzer, so that unless the height of the pulse from the counter lies within the range required to trigger the single channel discriminator, no count will be recorded. This feature is necessary in practice a) to permit a reliable and reproducible absolute calibration of the counting efficiency to be made, and b) to permit the rejection

of background pulses due to low energy neutrons and gamma rays - in order words to improve the signal-to-noise ratio. In certain cases, for example the study of the ($C^{13}(He^3,n)O^{15}$) reaction, which has a large Q and a low cross section, this feature has proved quite necessary.

Results: Time Resolution

The system has been used for a number of angular distribution and cross section measurements during the past year. Among these are $C^{12}(d,n)N^{13}$, $C^{13}(d,n)N^{14}$, $C^{12}(He^3,n)O^{14}$, $C^{13}(He^3,n)O^{15}$, $C^{13}(a,n)O^{16}$, and $Be^9(a,n)C^{12}$.

Results obtained in the last of these after careful adjustment of the cyclotron are shown in Figure 8. One channel is equivalent to about one millimicrosecond. Curves are shown for several settings of the attenuator in the slow pulse height discriminator line. The full width of the lines at half maximum is about 2 ns in this favorable case. Generally the widths have ranged from approximately this to about 3.5 ns, although it is easily possible to do worse by using incorrect stop signal pulses, or too low photomultiplier voltage, etc. It should be noted that the thickness of the scintillon neutron detector used in these measurements was 1", which made the counting efficiency high, but contributed appreciably to widening the peaks. The flight time of a 5 Mev neutron through the detector is about 0.8 ns, for example.

Figure 9 shows the effect of increasing the cutoff energy for counting, E_o, on the neutron spectrum from the $Be^9(d,n)$ reaction.

Most experiments have been made with flight paths less than 1.2 meters long in order to avoid difficulty with neutrons scattered from the solid concrete floor, which is four feet below the beam pipe. Within that range the neutron counter can be used unshielded. A massive lead and lithium hydride - loaded paraffin shield is available for use either with the standard 2" counter or with a 5" one. Its use removes most of the floor scattering, but it has not been expolited in any important way, partly because we have not yet determined what effect the shield has on the counting efficiency of the neutron detector.

Absolute Counting Efficiency

For the experiments mentioned above a knowledge of absolute counting efficiency of the system was required. Calibration curves were obtained by use of the $D(d,n)$ reaction, the cross sections for which are known to 4% accuracy.* In addition, an early experiment on the $C^{12}(d,n)N^{13}$ was used in a check on the calibration. The angular distribution of the neutrons obtained with 3.02 Mev deuterons was measured and the total yield of neutrons was determined by integrating under the angular distribution curve. Then a second experiment was performed in which the yield of annihilation radiation from the N^{13} decay positrons was compared with the known flux of annihilation radiation from a sodium 22 source calibrated at the Bureau of Standards. A coincidence counter setup was used for these measurements. Results obtained in this way agreed to within 10% with expectations from the absolute calibra-

*Los Alamos Report 2014.

tion of the neutron detector.

In the early experiments the pulse height discriminator in the start channel of the converter unit was used to fix the threshold for counting.* Usually the dial was set to the most sensitive position in order to obtain the highest counting efficiency and, more importantly, to maintain good time resolution. It soon became apparent that a system of pulse height discrimination separate from the fast timing circuits was highly desirable. Then the slow discriminator circuit was added.

Calibration curves were obtained for various settings of the attenuator in the slow discriminator channel, but first a method was worked out to make possible resetting the apparatus after a shutdown so that the calibration curves would be reproduced, even though conditions had changed somewhat; for example the sensitivity

---

* In the course of experiments on pulse height discrimination we found that our fast transistor trigger circuit did not respond in the same way with proton recoil pulses as with electron pulses. Apparently the emission of light in the case of protons lasts slightly longer, and the trigger circuit responded more sensitively to the longer pulses. Apparently also the tail on the pulses comes chiefly from slow-moving protons. This is a well known effect in organic scintillators, especially in stilbene where it has been used as the basis for pulse shape discrimination of particle types with circuits designed especially for that purpose.

of the photomultiplier tube might have changed, possibly because of voltage changes. The problem was to set the continuously variable slow discriminator dial so that the level of discrimination would correspond to a certain standard light signal from the scintillator. A Cs^{137} source was used as a standard. The discriminator level was set to correspond to the peak in the observed γ-ray pulse height spectrum. Figures 10 and 11 show some measured efficiency curves.

Our counter was a piece of scintillon, polyvinyl toluene, C_9H_{10}, 2" in diameter and 1" long. In principle one can calculate the counting efficiency of the detector, given its chemical constitution, its geometry, and the cutoff energy for counting. A full treatment would be very complicated because of the variety of processes besides simple n-p scattering which may occur, for example elastic and inelastic scattering from carbon, $C^{12}(n,p)$ and (n,α) reactions, etc.[2] However, under usual conditions it seems that most of the complicating processes are unimportant. In the case of inelastic scattering from carbon gamma rays emitted in nuclear de-excitations may give an additional contribution to counting, but this will be small. Elastic and inelastic scattering deflect the neutrons, changing their path lengths, but for our

---

2. Fast Neutron Physics. Interscience Publishers. New York (1960); J. C. Belote, Sandia Corporation Monograph SCR-467 (1962); R. Batchelor, W. B. Gilboy, J. B. Parker, J. H. Towle, The Response of Organic Scintillators to Fast Neutrons (privately circulated monograph to be published in Nuclear Instruments and Methods).

detector geometry this sometimes produces longer parths, sometimes shorter, with the result that the average path length isn't changed greatly. It turns out that the efficiency can be calculated with satisfactory accuracy on the assumptions (i) that only n-p scattering is effective, (ii) that only single scattering is important, and that any single scattering event producing a proton of recoil energy greater than the slow discriminator cutoff value will produce a count, (iii) that the effective length of the counter is its geometrical length, and (iv) that the recoil protons have negligible range compared with the dimensions of the counter. The result is

$$\epsilon = \text{efficiency} = \left(1 - \frac{E_o}{E_n}\right)\left(e^{-n_H \cdot \sigma_{np} \cdot \ell}\right) \qquad (1)$$

where E_n is the energy of the neutron entering the detector, E_o is the threshold energy of a neutron for counting, n_H is the number of hydrogen nuclei per cm^3 in the target, σ_{np} is the total n-p scattering cross section for a neutron of energy E_n, and ℓ is the length of the counter. The first factor in (1) is exact. It does not depend on the exact shape of the response curve (pulse-height vs proton recoil energy) of the scintillator. However E_o must be found for each setting of the slow discriminator. The best way we have found to do this is to obtain a check occasionally using the D(d,n) reaction to get the response of the system to a known number of neutrons, then using Eq. (1) to find E_o. The cross section $\sigma_{np}(E_n)$ is conveniently calculated from Gammel's semi-empirical formula

$$\sigma_{np}(E_n) = \frac{3\pi}{1.206\,E_n + (-1.86 + 0.094\,E_n + 0.0001306\,E_n^2)^2} + \frac{\pi}{1.206E_n + (0.4223 + 0.13E)^2} \quad (2)$$

which is said to be accurate to several parts in 10^3 up to 42 Mev.[3]

Beam Pulse Scaling

Beam pulses emerge from the cyclotron at a frequency ranging from 10 to 20 megacycles. Sometimes it is convenient to have a lower beam pulse frequency, for example when working at the low energy end of a neutron spectrum, especially when a long flight path is involved. The problem is to prevent any faster neutrons from a later beam pulse from catching up with or passing, the slower neutrons and being confused with them in the spectrum. In our case reducing the frequency of beam pulses to about 3 mc can virtually eliminate the problem.

We have therefore constructed a beam pulse scaler which provides electrostatic deflection of the beam bunches in the beam pipe at a subharmonic of the cyclotron frequency so that only one bunch in three, say, reaches the target. The first version of the scaler was rather crude -- although it worked. A second version, which has been tested on the bench but has not been used, is now

---

3. W. D. Allen. Neutron Detection. Philosophical Library Inc., New York (1960).

described. It is a refined version of the first.

In order to simplify tuning procedures the scalar system was designed with a minimum of tuned circuits: there is only one, the tank circuit associated with the beam deflection plates. There are two main units, a frequency divider and an amplifier which drives the deflection plates.

The frequency divider (Fig. 13) is a low powered circuit driven by a signal picked up from the cyclotron oscillator. It consists of a multivibrator locked in to operate at a subharmonic of the frequency of the cyclotron oscillator. Its output is amplified by a one stage amplifier which feeds into a cathode follower output stage. The power amplifier (Fig. 14) contains two untuned amplifier stages which drive a pair of 807's in the output stage. The tank circuit of the output stage is the deflection plate circuit, the only tuned circuit in the system.

In bench tests the system has performed very satisfactorily. The frequency divider could be locked in stably on a 2 to 200 volt signal of frequency ranging from 5 to 25 mc obtained from a test oscillator. The range of multivibrator frequencies for satisfactory operation is 2 to 5 mc. In practice we expect to operate the system at one third the oscillator frequency in the range from roughly 10 to 15 mc, which means that the scaled beam pulse frequency will range from 3.3 to 5 mc. For cyclotron frequencies above 15 mc we will use a higher scaling ratio, possibly 1:5, which will give a scaling factor of 5. We might also choose 1:6,

which would again lead to a scaling factor of 3, since in this case (even subharmonic) beam pulses will arrive at the deflection plates at both zeros of each cycle of the deflection voltage, not just one, as in the case of odd ratios.

When the original beam pulse scaler was used, a scintillation detector served to generate the reference pulses, so scaling the beam pulses made no essential difference with respect to stop pulse generation. However, with the present arrangement of stop pulse generation based on the cyclotron oscillator voltage the situation is more complicated. This can be illustrated by assuming, for definiteness that $f_{scaled} = 1/3\ f_{cyc}$. Then there are three stop pulses generated per beam pulse striking the target. Ideally only one of the three should be allowed to reach the converter unit, and from one beam pulse to the next the chosen stop pulse should always have the same phase with respect to the arriving beam pulse. The obvious way to secure this result is to make use of the subharmonic signal in some manner, but in order to preserve accuracy of timing it is probably best to use stop pulses based directly on the cyclotron oscillator. Therefore we expect to use a signal from the output of the frequency divider to open a gate circuit, which will then transmit the next arriving stop pulse to the converter unit. This can be done with a gate unit similar to that of Figure 6, shown in Fig. 15, or by simply modifying that circuit to include a second 6688 gate tube with its plate connected to the same diode, and its grid controlled by the output signal

from the frequency divider. One would then have a coincidence circuit which would transmit a stop pulse only if there had been a neutron counter pulse and also only if it was the correct one of the group of three possible stop pulses in the subharmonic cycle.

Acknowledgment

Dr. Charles Frei, now at the University of Zurich, participated at an early stage in the development of the equipment described here, especially in the construction of an early version of the transistorized converter and in testing the feasibility of using a parasitic scintillation counter, in the beam pipe, to generate the stop pulses.

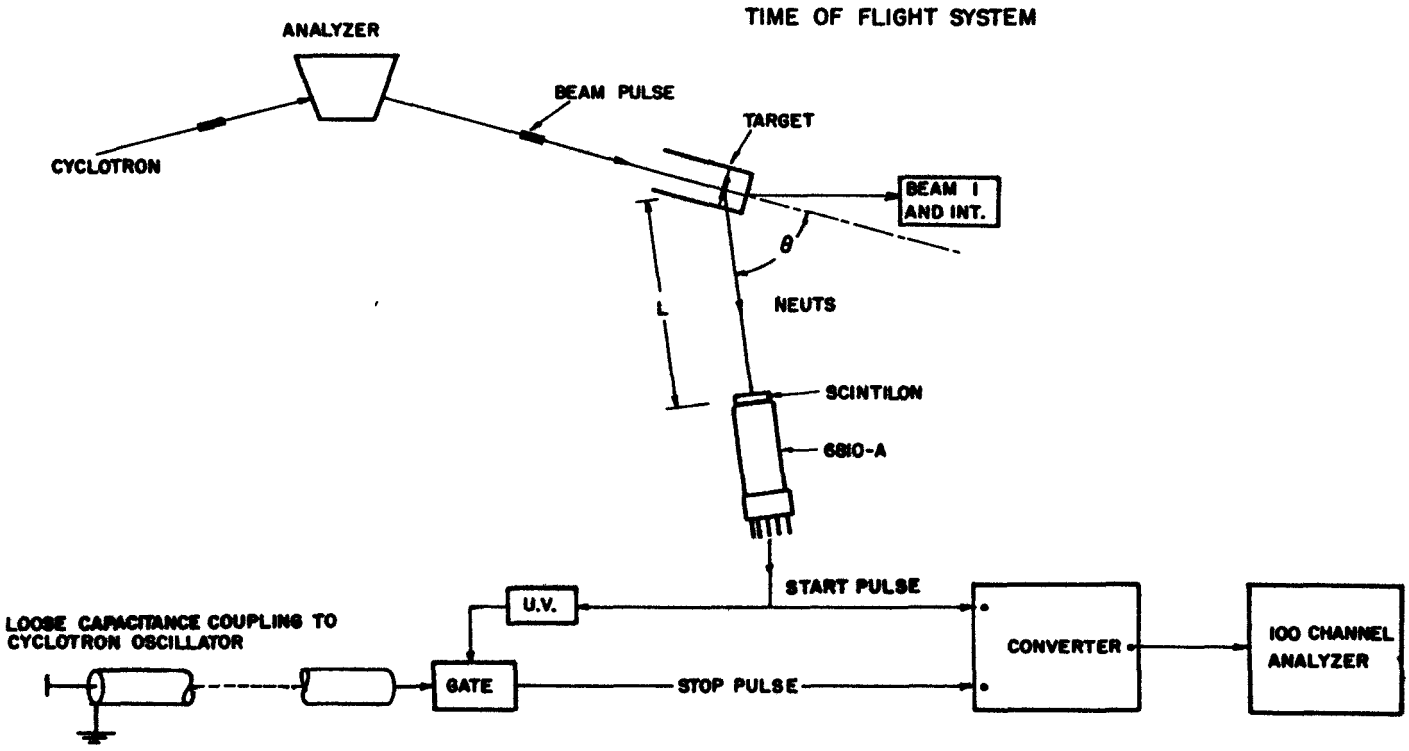

Fig. 1. Overall Diagram of Time of Flight System.

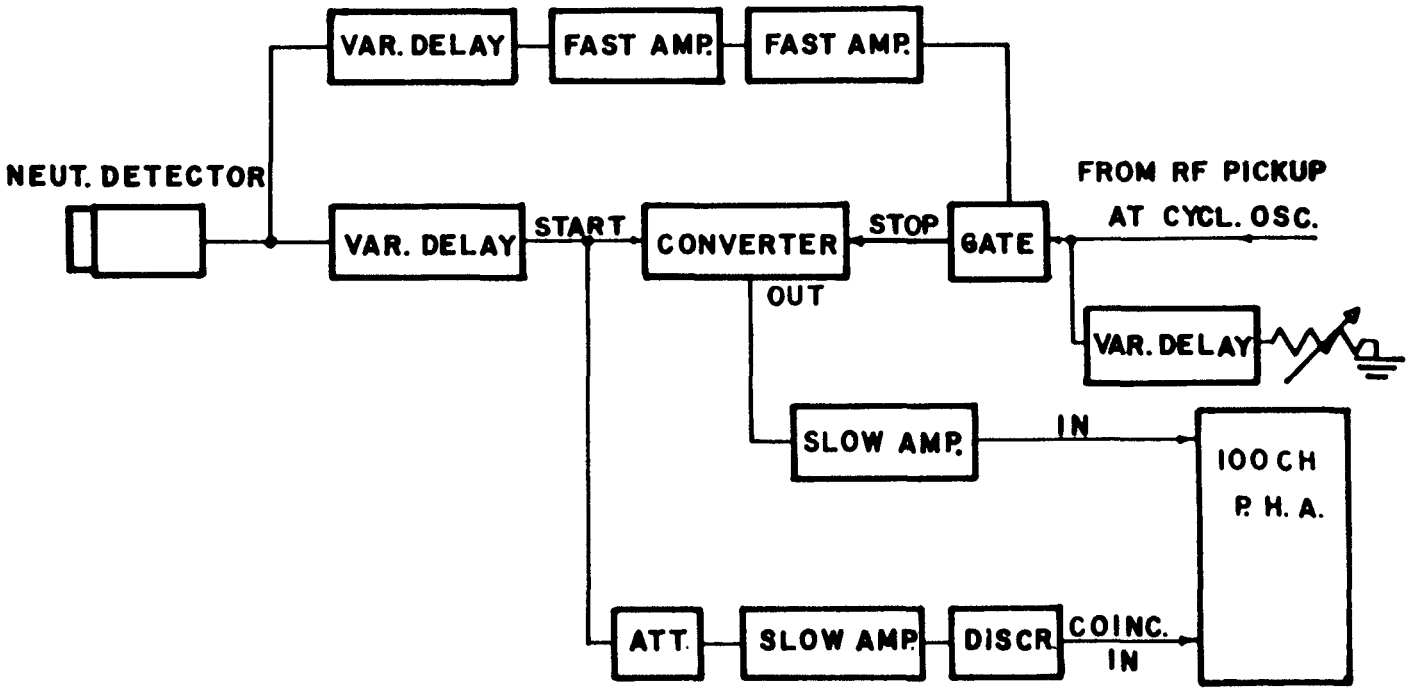

BLOCK DIAGRAM OF TIME OF FLIGHT SYSTEM

Fig. 2. Block Diagram of Electronic Circuits of the Time of Flight System.

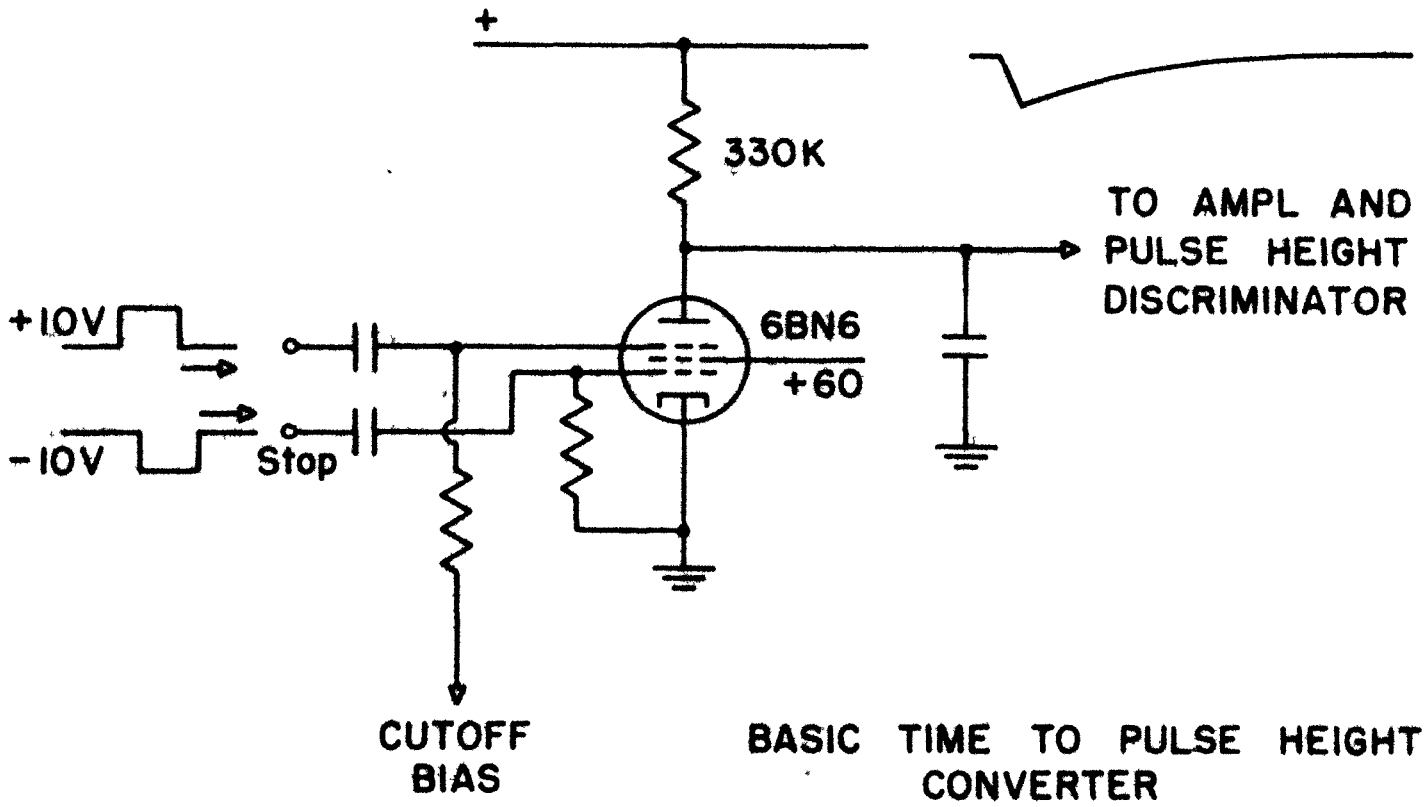

Fig. 3. Principle of the Time to Pulse Height Converter.

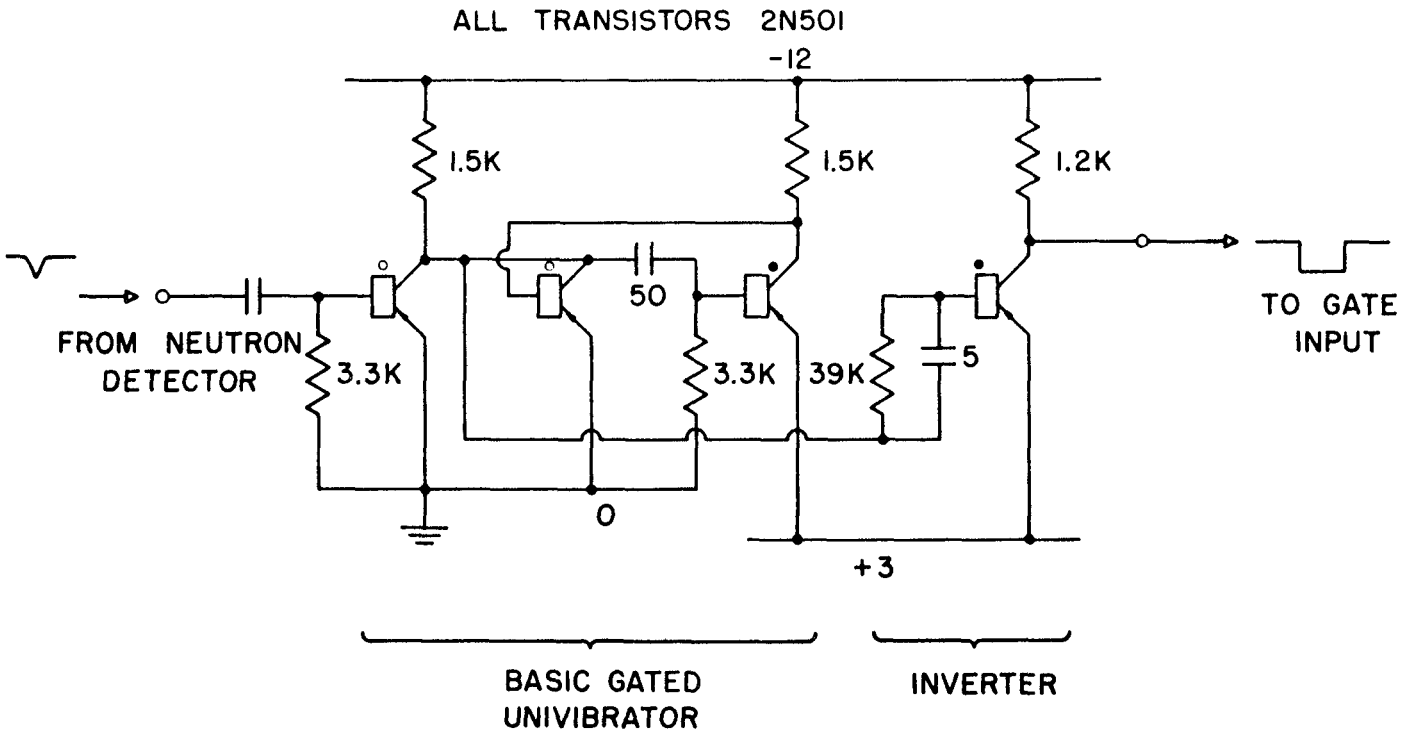

Fig. 4. Basic Triggered Univibrator Circuit.

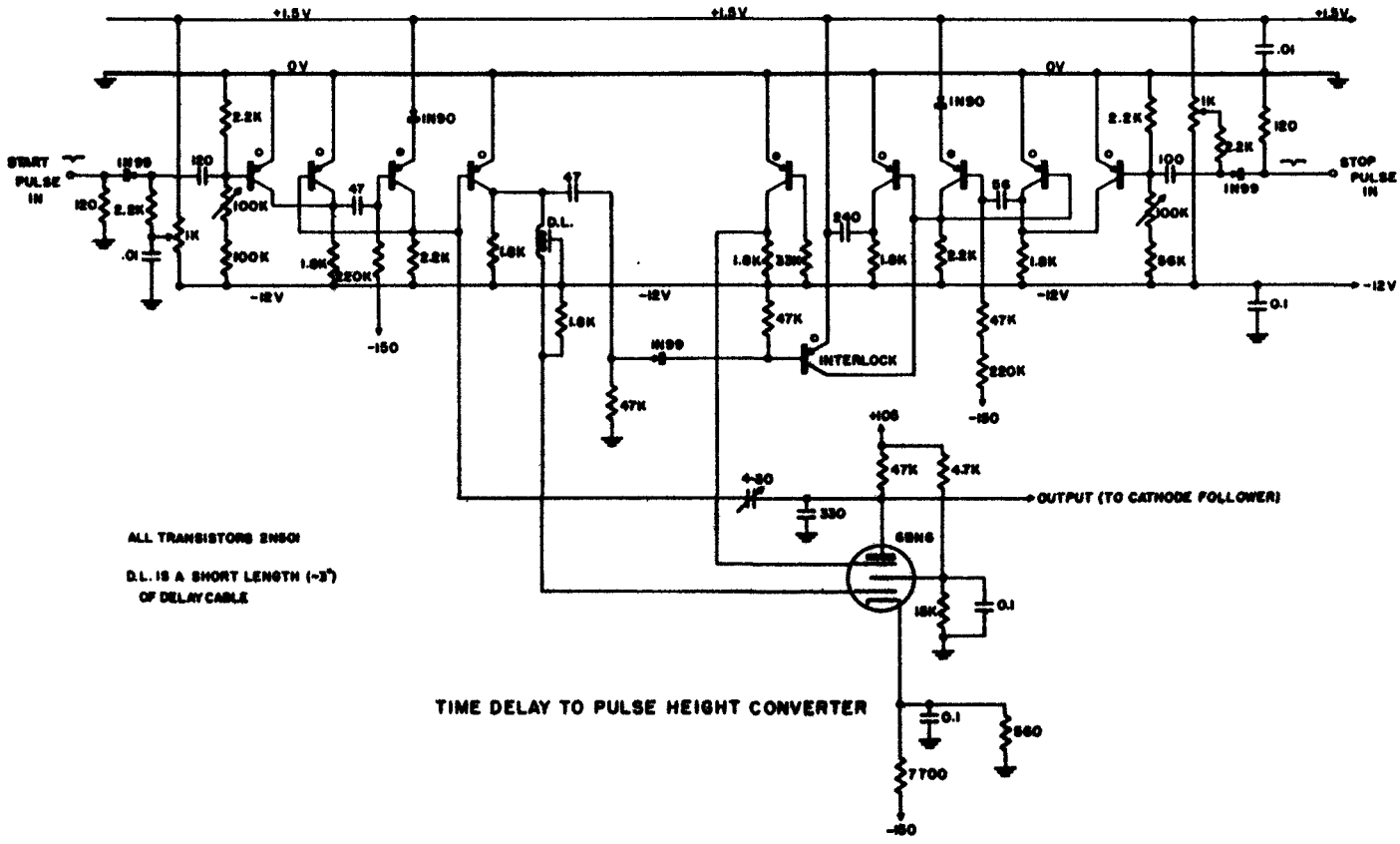

Fig. 5. The Time to Pulse Height Converter Circuit.

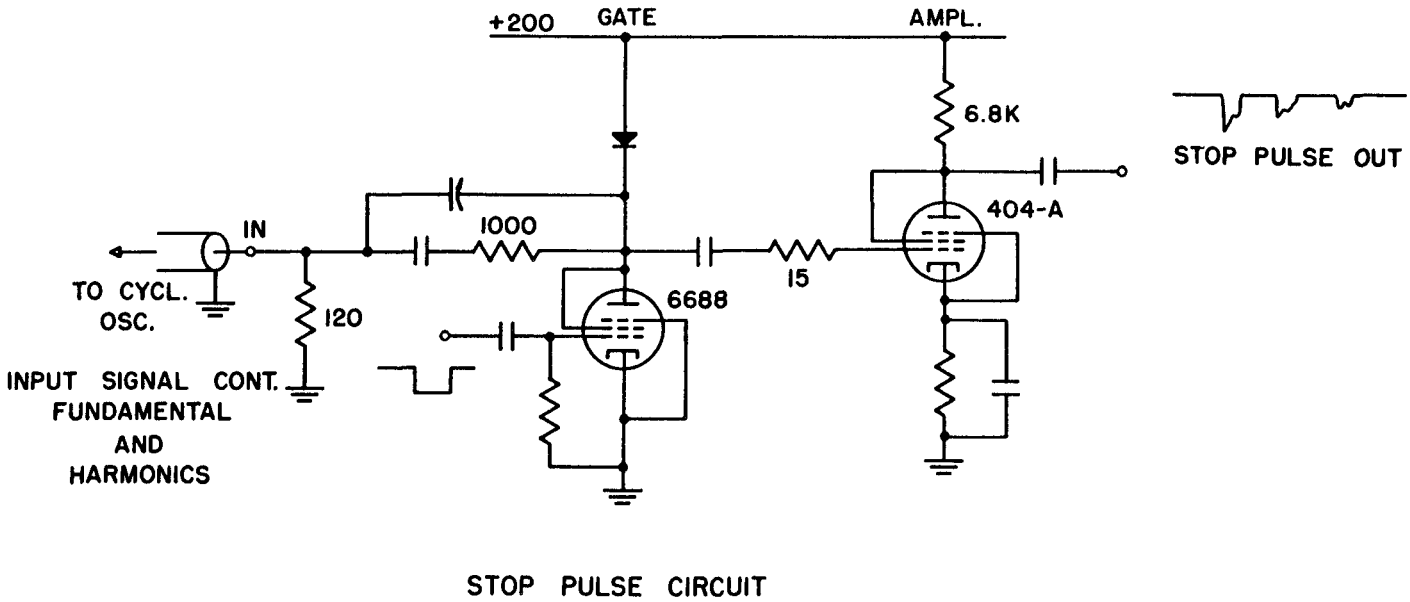

STOP PULSE CIRCUIT

Fig. 6. Stop Trigger Pulse Generator. Shunting cable stub not shown: See Fig. 2 and text.

(a)

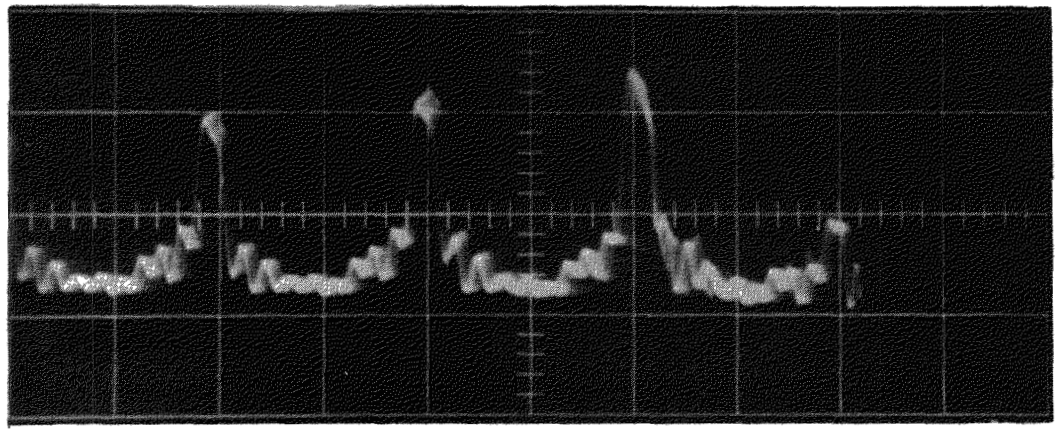

(b)

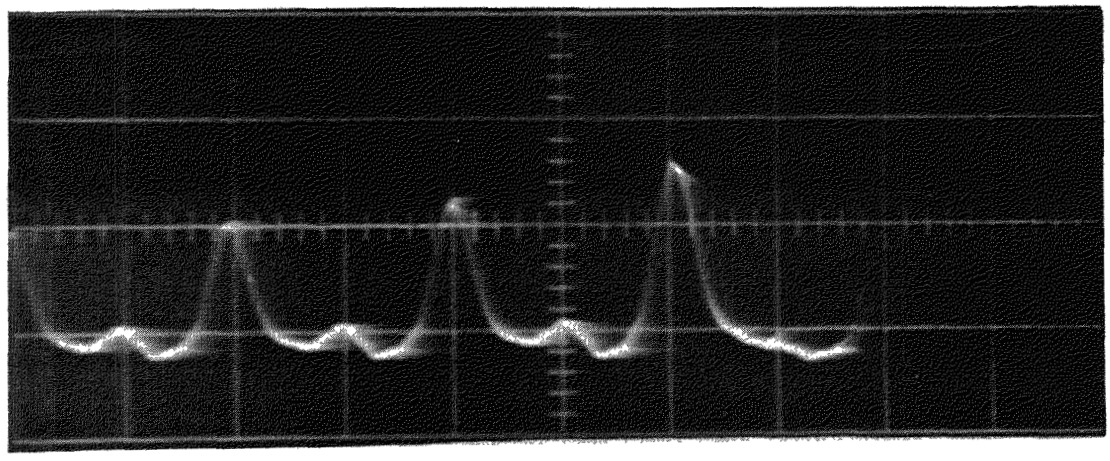

(c)

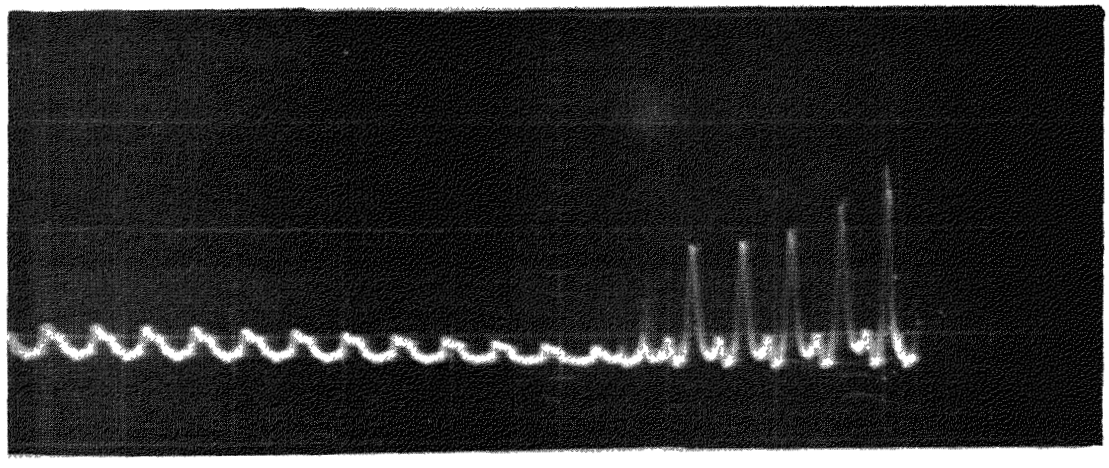

Fig. 7. Examples of Stop Pulses. Time runs from right to left. Sweep speed 50 ns/cm. a) Observed with fast conventional oscilloscope. b) With slower oscilloscope. c) Same, but with 250 ns/cm sweep speed.

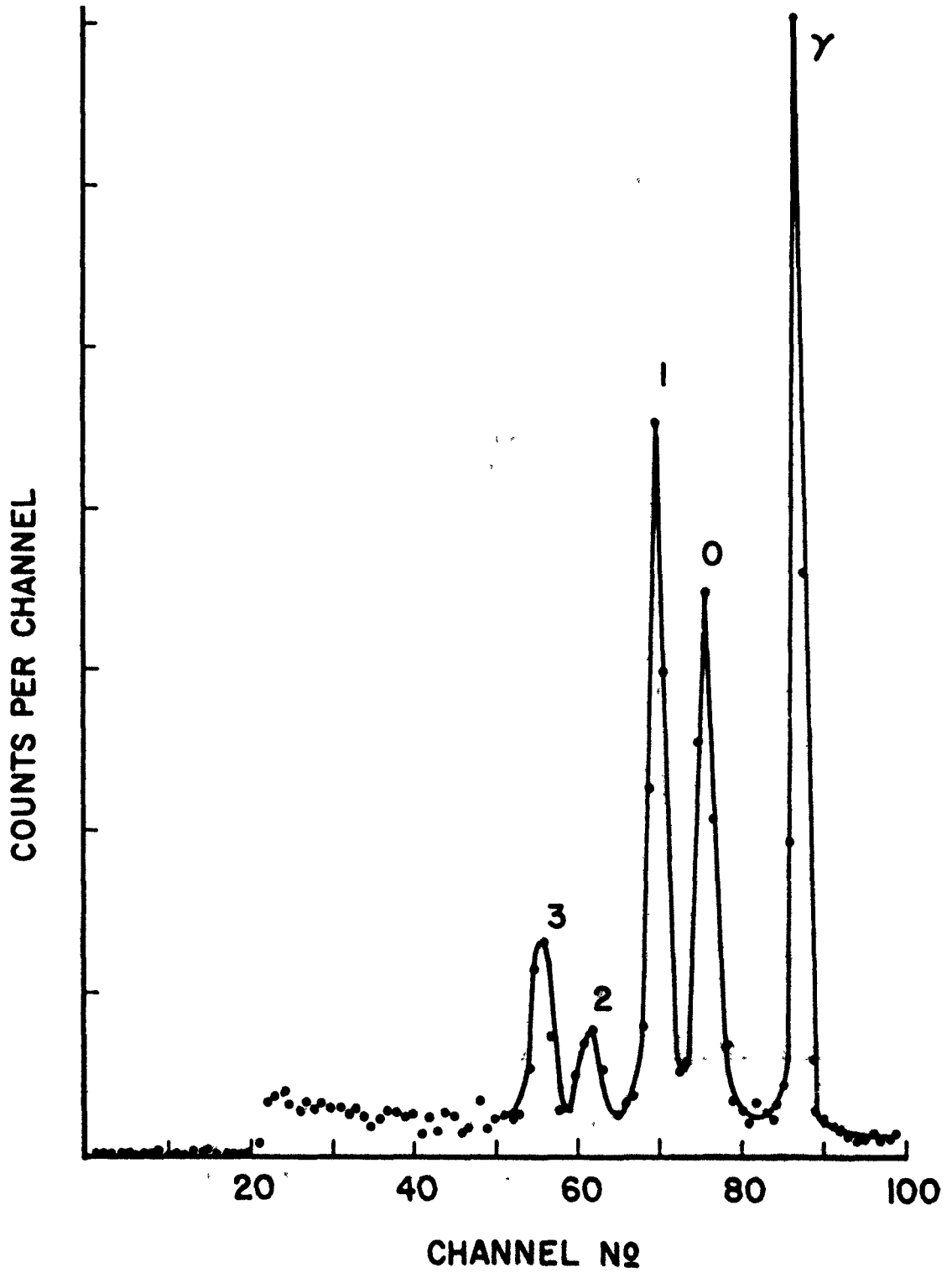

Fig. 8. $Be^9(\alpha,n)$ Spectrum.

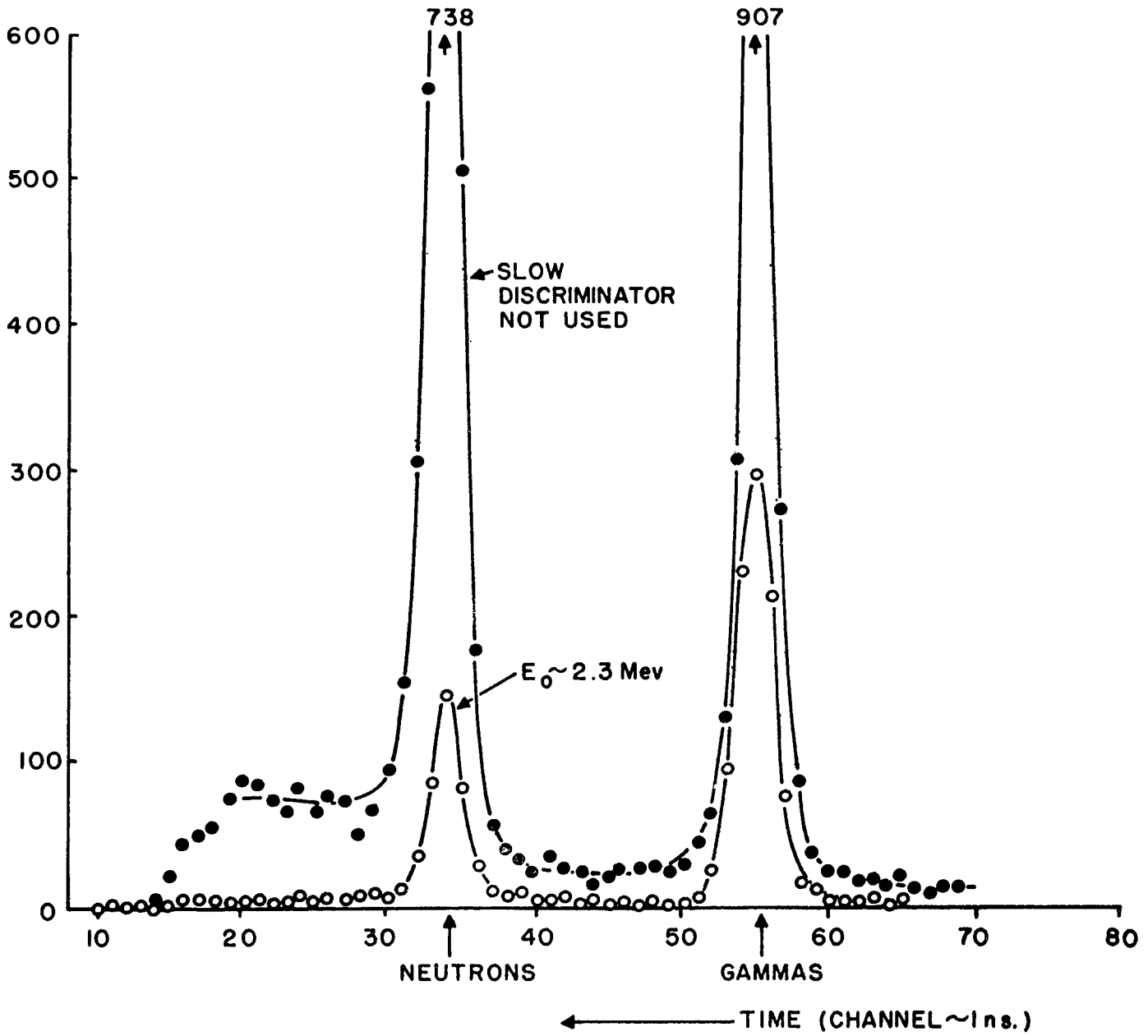

Fig. 9. Effect of E_o on the Observed $C^{12}(d,n)$ Spectrum. More striking improvements are usually observed with higher neutron energies and higher E_o.

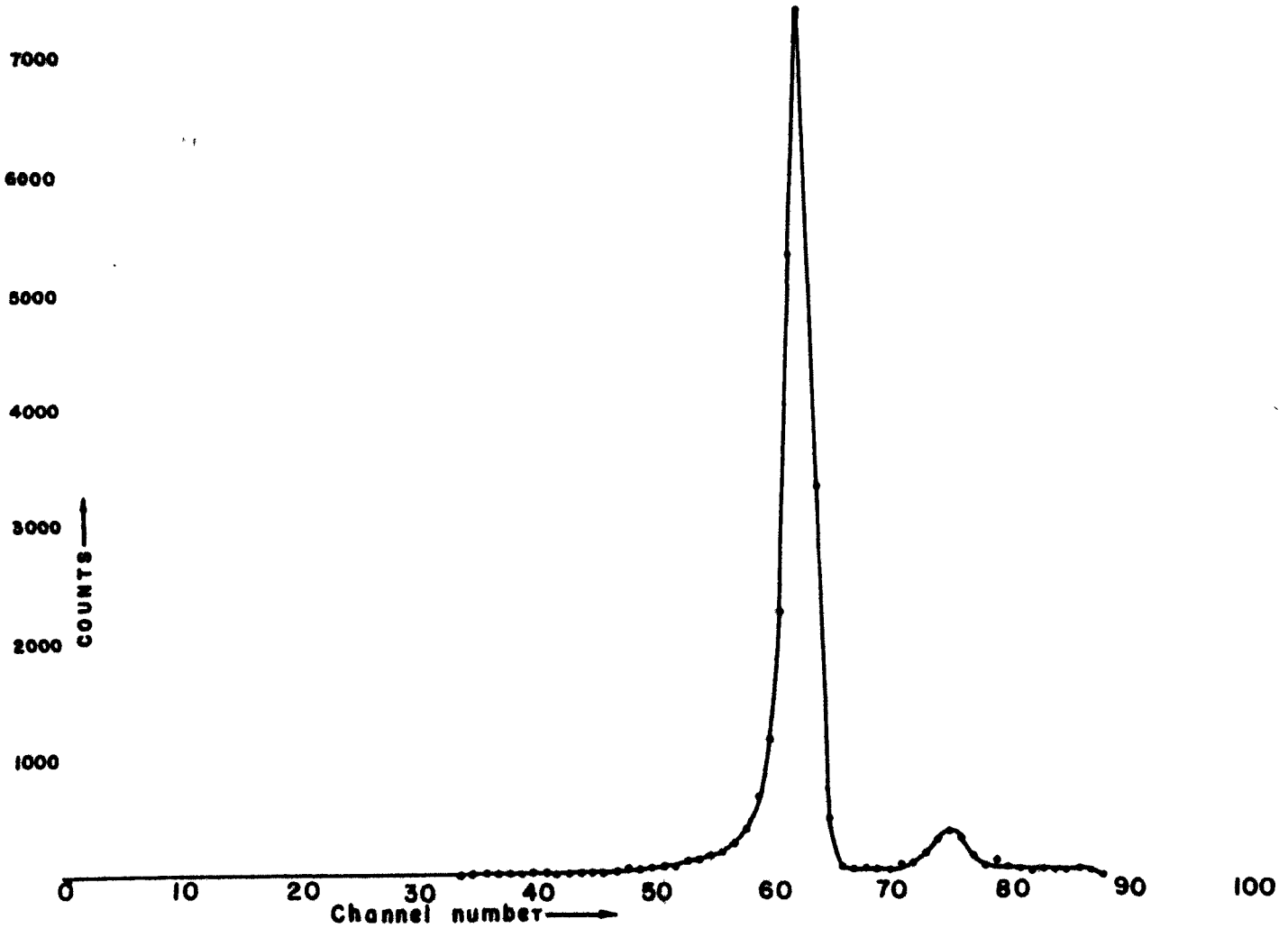

Fig. 9a. D(d,n) Spectrum. Left peak, neutrons. Right peak gammas. Slow discriminator not used. Notice tailing at low energy side caused by the smaller neutron counter pulses. Use of slow discriminator with E_o set at several Mev would eliminate the tail.

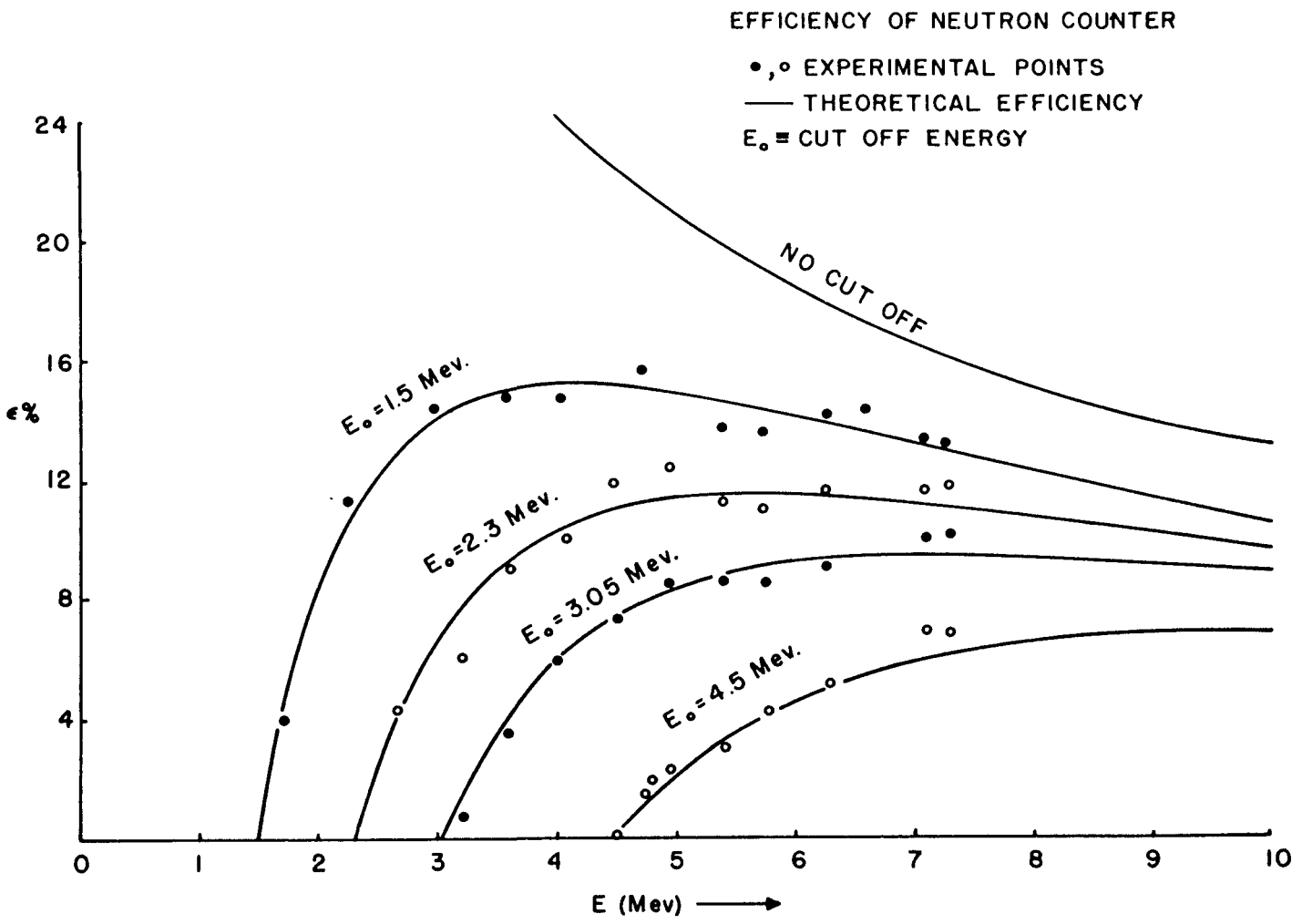

Fig. 10. Experimental Efficiency Points Compared with Theoretical Curves for Various Values of the Neutron Cutoff Energy E_o. Relative efficiencies for E_n up to 14 Mev (not plotted) also agree well with the theoretical curves.

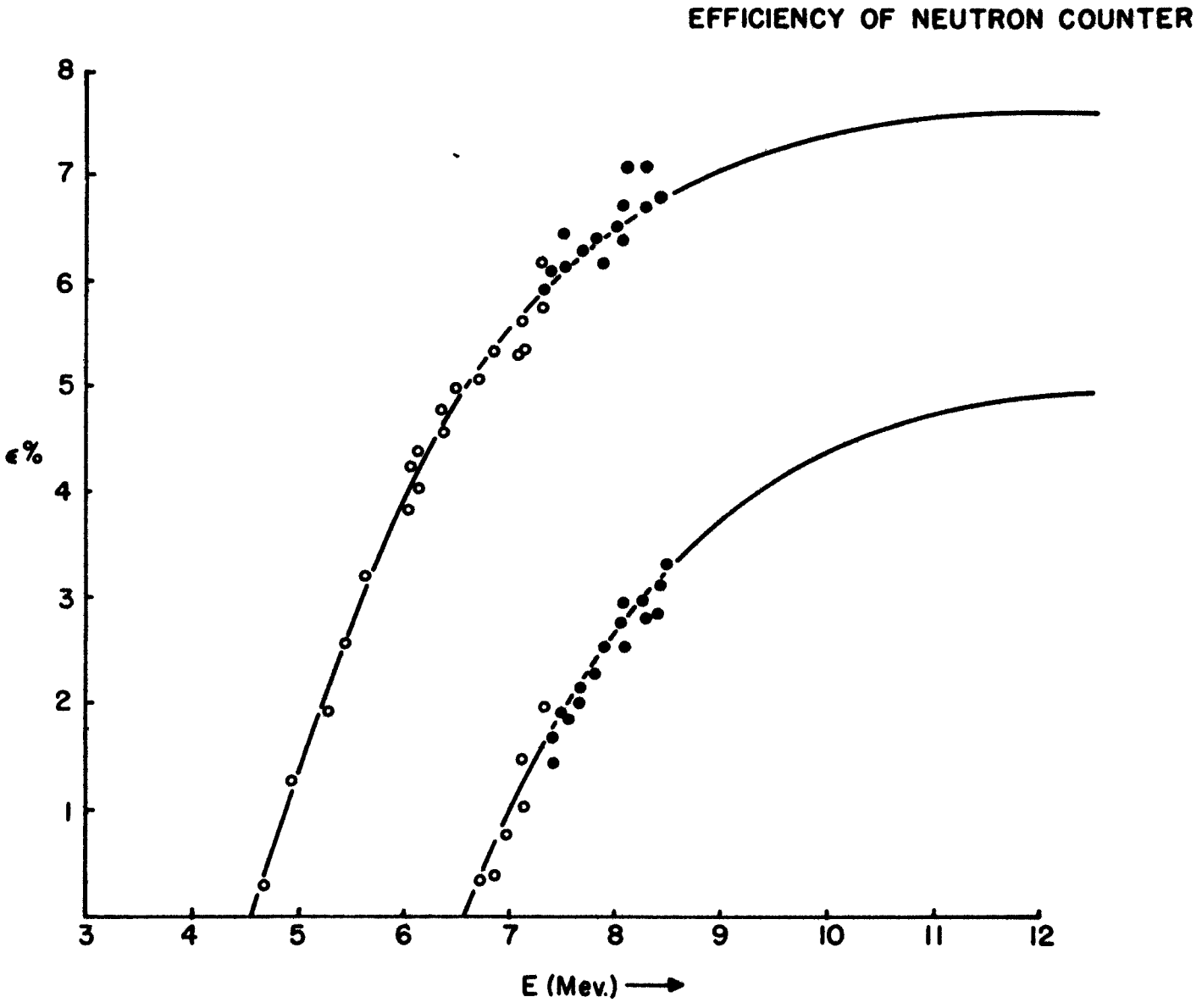

Fig. 11. A Set of Efficiency Curves. Circles, absolute measurements; solid points, relative values (normalized to fit the circle points on one curve); the curves, calculated from Eq. (1).

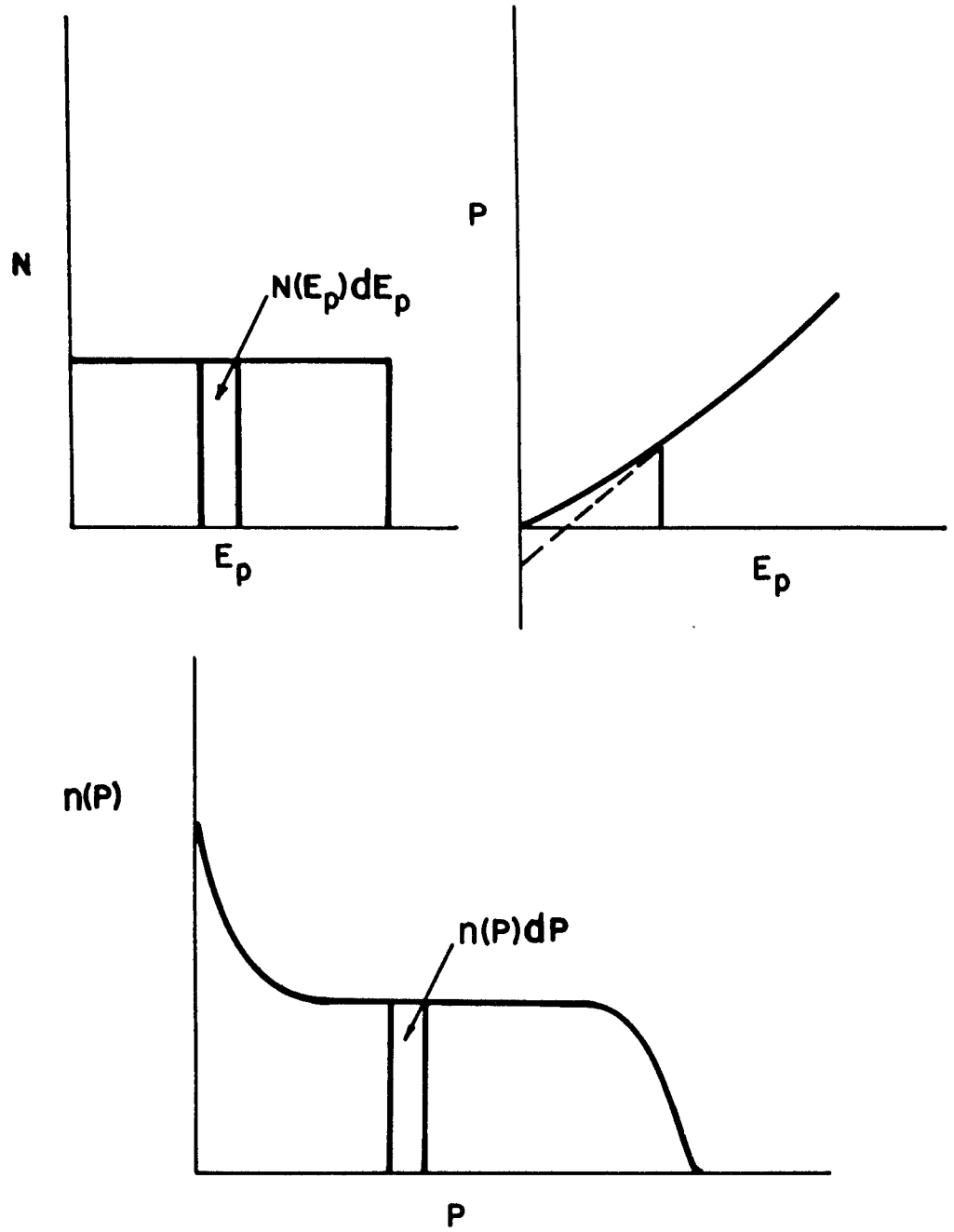

Fig. 12. Upper Left, Theoretical Spectrum of Recoiling Protons from Bombardment of Hydrogen with Monoenergetic Neutrons. Upper Right, Pulse Height, P from Scintillon Counter vs. Energy E_p of Recoil Proton. Lower, Type of Spectrum of Pulses Actually Observable for Monoenergetic Neutrons. The departure from the theoretical spectrum is due to the nature of the response curve of scintillon and to statistical effects. The factor $(1 - \frac{E_0}{E_n})$ in (1) depends upon the flatness of the recoil spectrum and is independent of the shape of the response curve, so long as it is monotonic.

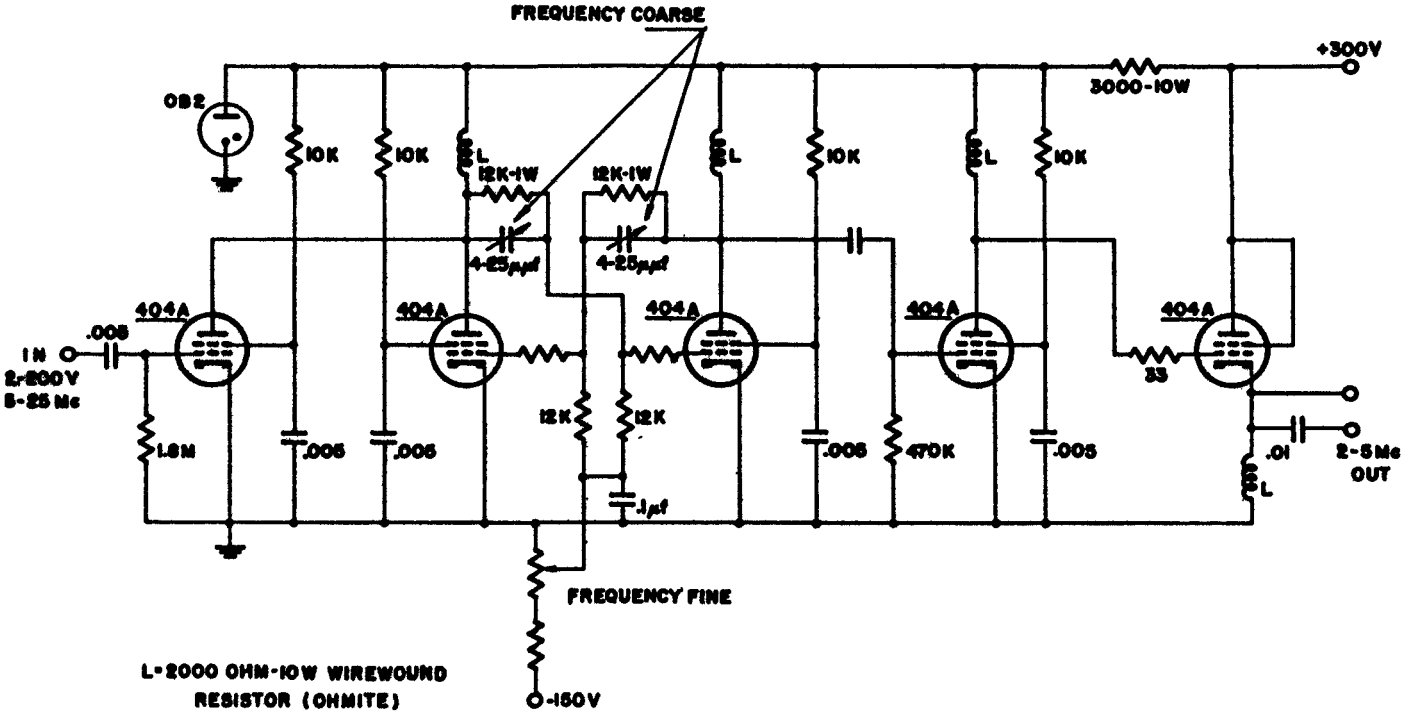

Fig. 13. Diagram of Frequency Divider Used in Beam Pulse Scaler.

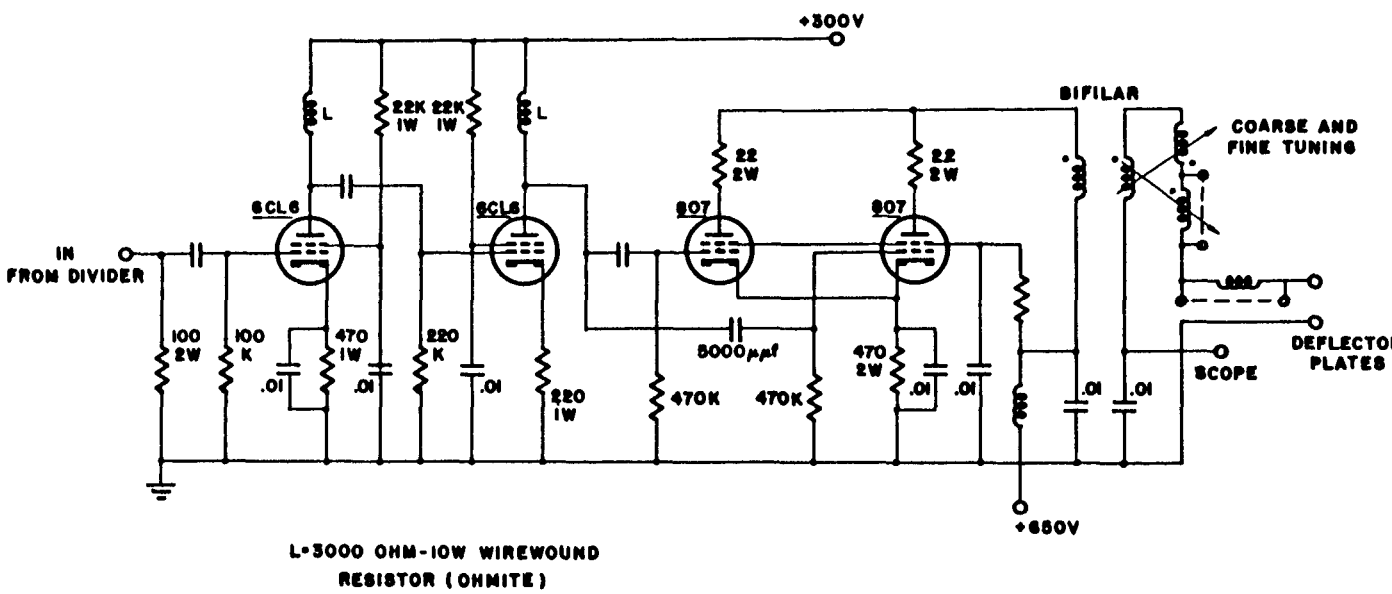

Fig. 14. Diagram of Power Amplifier of Beam Pulse Scaler.

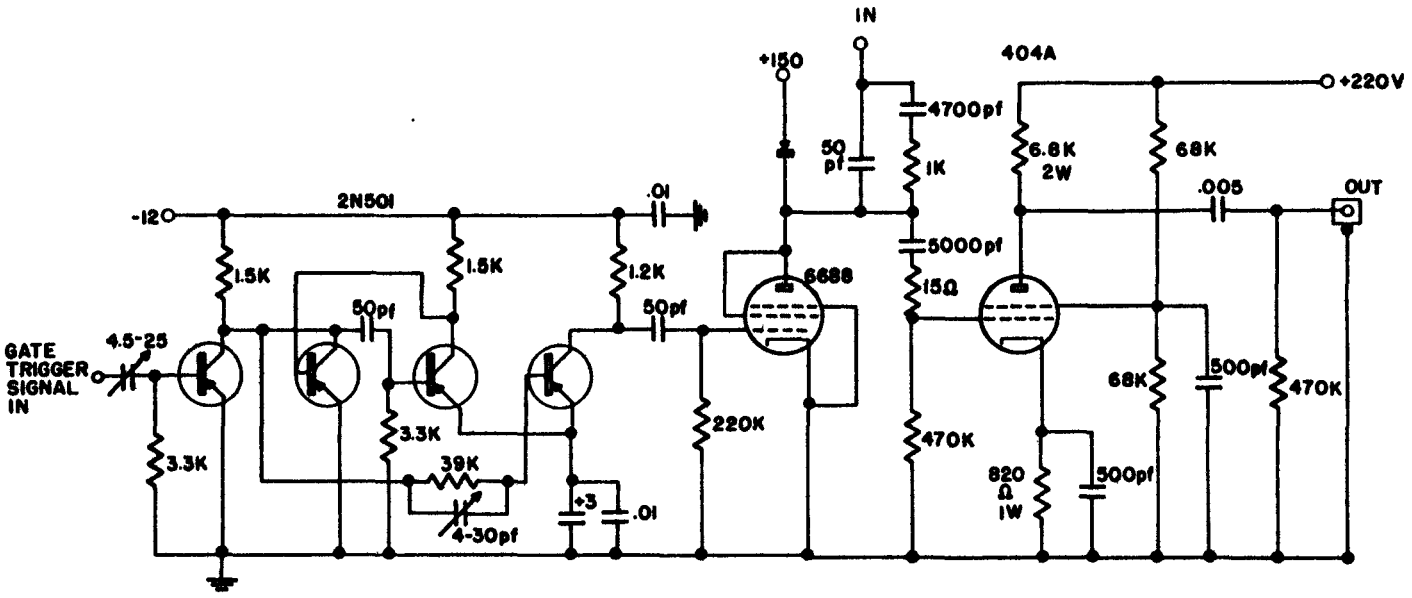

FAST GATE CIRCUIT

Fig. 15. Gate Circuit for Possible Use in Beam Pulse Scaler System to Obtain the Correct One (of Three) Stop Pulses in a Subharmonic Cycle. (The beam pulse scaler system has not yet been used.)